Geomechanics and Engineering, *Vol. 10, No. 4 (2016) 437-454*
DOI: http://dx.doi.org/10.12989/gae.2016.10.4.437

A fully coupled thermo-poroelastoplasticity analysis of wellbore stability

Xiaohua Zhu *, Weiji Liu [a] and Hualin Zheng

School of Mechatronic Engineering, Southwest Petroleum University, Chengdu 610500, China

(*Received April 21, 2015, Revised December 25, 2015, Accepted January 07, 2016*)

Abstract. Wellbore instability problem is one of the main problems that met frequently during drilling, particularly in high temperature, high pressure (HPHT) formations. There are large amount of researches about wellbore stability in HPHT formations, which based on the thermo-poroelastic theory and some achievements were obtained; however, few studies have investigated on the fully coupled thermo-poroelastoplasticity analysis of wellbore stability, especially the analysis of wellbore stability while the filter cake formed. Therefore, it is very necessary to do some work. In this paper, the three-dimensional wellbore stability model which overall considering the effects of fully coupled thermo-poroelastoplasticity and filter cake is established based on the finite element method and Drucker-Prager failure criterion. The distribution of pore pressure, wellbore stress and plastic deformation under the conditions of different mud pressures, times and temperatures have been discussed. The results obtained in this paper can offer a great help on understanding the distribution of pore pressure and wellbore stress of wellbore in the HPHT formation for drilling engineers.

Keywords: wellbore stability; numerical simulation; filter cake; temperature; permeate; fully coupled

1. Introduction

Wellbore instability problems include blowout, lost circulation, stuck tools and wellbore collapse et al., the accidents caused by wellbore instability result in serious drilling safety and quality problems. More than six billion dollars are spent in controlling wellbore instability every year in the global petroleum industry and wellbore failures give rise to significant lost time accounting for over 40% of all non-productive time according to the statistics (Wu *et al*. 2009, Zhang *et al*. 2009, Zhu and Liu 2013). The wellbore stability problem becomes more complex especially in HPHT formations owing to the fully coupled effects of in-situ stress, mud pressure, pore pressure and temperature. Therefore, it is vital to understand the mechanisms of wellbore instability and analyze the reason of wellbore instability for insuring the safety during drilling and high rate of penetration and efficiency.

During the drilling process, the temperature gradients between the drilling mud and formation can significantly change the stress and pore pressure distributions nearby the borehole. Many researches have performed numerous studies about the wellbore stability while under the effect of

*Corresponding author, Professor, E-mail: zxhth113@163.com
[a] Ph.D. Student, E-mail: lwjzq1111@163.com

http://www.techno-press.org/?journal=gae&subpage=7 ISSN: 2005-307X (Print), 2092-6219 (Online)

coupled thermo-poroelastic. The extension of Biot (1941) theory for coupling thermal, hydraulic and mechanical processes in a fluid saturated porous media has caught the attention of many investigators, among them, Rice and Cleary (1976), Detournay and Cheng (1988), Cui *et al*. (1997, 1999), Cui *et al*. (1998), and Santarelli *et al*. (1986). Constitutive equations for thermo-poroelastic theory first introduced by Palciauskas and Domenico (1982) by extending the classic Biot's poroelastic theory for the nonisothermal case. Wang and Dusseault (2003) apply conductive-convective thermo-poroelastic theory to analyze wellbore stability in hot and cold water injection wells. A powerful wellbore stability model which includes poroelastic, chemical and thermal effects has been presented by Chen *et al*. (2003). The results using this model are presented by values of pore pressure, rock failure status and critical mud density. Chen and Ewy (2004) researched the thermo-poroelastic effect on wellbore stresses in permeable rocks. The fully coupled temperature and pore pressure are decoupled in diffusivity equations for a high-permeability rock and the solutions for temperature and induced stresses are analytically determined. Chen and Ewy (2005) presented the consistency of thermal effects between two available models for inclined borehole and studied the thermal effects for both a permeable and an impermeable boundary. Shahabadi *et al*. (2006) developed a thermo-poroelastic model that accounts for the effect of convective heat transfer and researched the effects of temperature and pressure changes on wellbore stability. Wang *et al*. (2007) established a porous elastic model which coupled the temperature and pore pressure and researched the pore pressure distribution nearby the wellbore. Sheng *et al*. (2008, 2009) presented a coupled thermo-poroelastic model in a saturated linear thermoelastic medium and a 2-D coupled thermo-poroelastic problem of a wellbore with known analytical results is simulated by using a FEMLAB-based simulator. Muller *et al*. (2009) have focused on the evaluation of the three-dimensional borehole response, particularly of the plastic zone, taking into account the spatial variability of both hydraulic and mechanical properties. Zhai *et al*. (2009) established a new model which integrated the effects of both thermal and hydraulic diffusion in determining the effects of the drilling fluid and mud weight on the borehole system to study the effects of poro-elasticity and thermo-elasticity on borehole stability. Tao and Ghassemi (2010) have studied the thermo-poroelastic effects on borehole failure and their impact on wellbore stability and the estimations of the in situ maximum horizontal stress and rock strength using wellbore failure data are investigated. Gelet *et al*. (2012) presented a fully coupled finite element formulation for a thermo-poro-elastic dual porous medium under non-isothermal conditions for the borehole stability analysis. Jia *et al*. (2012) studied the coupled process of wellbore and discussed the influence pore pressure, temperature and stress between different coupled fields. Diek *et al*. (2012) developed a finite element model for the fully coupled processes consisting of thermo-poroelastic deformation, hydraulic conduction, thermal osmosis, heat conduction, pressure thermal effect and the interconvertibility of mechanical and thermal energy. Wang *et al*. (2014) obtained the change regularities of the temperature and pore pressure nearby the wellbore in the radial direction through solving the thermo-poroelastic model as well as the tangential stress of wellbore while underbalanced drilling. Gomar et al. (2014) employed a geomechanics model that is fully coupled to diffusive transport processes and used the two-dimensional finite element methods for the near wellbore simulation.

Although a large amount of researches have referred in the above, few studies have investigated on the fully coupled thermo-poroelastoplasticity analysis of wellbore stability, especially the analysis of wellbore stability while the filter cake formed; therefore, it is very necessary to do some research. In this paper, the three-dimensional wellbore stability model which overall considering the effects of fully coupled thermo-poroelastoplasticity and filter cake is established

based on the finite element method and Drucker-Prager failure criterion. The distribution of pore pressure, wellbore stress and plastic deformation under the conditions of different mud pressures, times and temperatures have been discussed.

2. Thermo-poroelastic theory and rock failure criterion

2.1 Thermo-poroelastic theory

As everyone knows, the formation temperature increases with its depth increases. Drilling fluid temperature is rising from the ground to the bottom, but it still lower than the bottom formation temperature; therefore, the wellbore rock matrix and pore medium will shrink due to the cooling effect on the wellbore wall. On the contrary, drilling fluid temperature is decreasing from the bottom to the ground and it is still higher than the upper formation temperature, the rock matrix and porous medium will be expanded because of the heating effect on formation. With the time increases, the affected zone cause by the temperature difference between drilling fluid and formation will become deeper. The schematic of the heat transfer and seepage process between drilling fluid and formation is shown in Fig. 1.

The governing equation considering the theory of thermo-poroelasticity includes the constitutive transport laws. The constitutive equation of rock skeleton is as follows

$$Gu_{j,ii} + (\lambda + G)u_{i,ij} - ap_{,j} - K_m \beta_m T_{,j} - f_j = 0 \tag{1}$$

The coupled energy and fluid mass balance equations can be written as

$$\begin{aligned} &\frac{k}{\mu}\nabla^2 p = \beta \frac{\partial p}{\partial t} - \alpha \frac{\partial \varepsilon_{kk}}{\partial t} + \beta_s \frac{\partial T}{\partial t} \\ &\rho_s c_s \frac{\partial T}{\partial t} + \rho_f c_f v \nabla T = k_s \nabla^2 T \end{aligned} \tag{2}$$

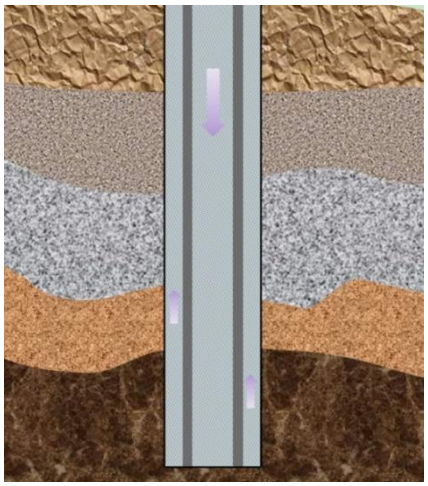

Fig. 1 The schematic of the heat transfer and seepage between drilling fluid and formation

The relevant parameters in Eq. (2) can be calculated with the following equations

$$\beta = \frac{\alpha - n}{K_m} + \frac{n}{K_f} \tag{3}$$

$$\beta_s = \alpha\beta_m + n(\beta_f - \beta_m) \tag{4}$$

$$\rho_s c_s = (1-n)\rho_m c_m - n\rho_f c_f \tag{5}$$

$$k_s = (1-n)k_m + nk_f \tag{6}$$

Where the p and T represent the pore pressure and temperature respectively. The constants α represents Biot coefficient. K_m is the drained bulk modulus of poroelastic matrix. K_f is the bulk modulus pore fluid. k_s is the means rock thermal conductivity coefficient. k_m is the thermal conductivity coefficient of rock skeleton. k_f is the thermal conductivity coefficient of pore fluid. β_m is the thermal expansivity of rock skeleton. β_f is the thermal expansivity of pore fluid. β is the Biot's modulus. β_s is the undrained thermal expansivity of saturated rock. k is the rock intrinsic permeability, $k = K{\cdot}\mu/\gamma_w$. μ is the fluid viscosity. c_f and c_m are the fluid and rock specific heat capacity. ρ_m and ρ_f mean rock skeleton and pore fluid density. f is the body forces, and the indices i,j stand for x and y coordinate axes. The coefficients λ and G are elastic moduli, known as Lame's parameters, v is darcy velocity, n is porosity, t represents time.

2.2 The failure criteria of rock

This paper considers the influence of elastoplasticity stresses on wellbore failure. The Drucker-Prager failure criterion which has considering the effects of intermediate principal stress and hydrostatic pressure has been used to determine whether shear failure occurs (Cai *et al*. 2002, Zhu *et al*. 2005, Chen *et al*. 2008)

$$F = m_a I_1 - \sqrt{J_2} + k_1 \tag{7}$$

In which I_1 and J_2 represent the first stress invariant and the second deviatoric stress invariant, respectively.

$$I_1 = \sigma_{rr} + \sigma_{\theta\theta} + \sigma_{zz} \tag{8}$$

$$J_2 = \frac{1}{6}\left[(\sigma_{rr} - \sigma_{\theta\theta})^2 + (\sigma_{rr} - \sigma_{zz})^2 + (\sigma_{\theta\theta} - \sigma_{zz})^2\right] + \sigma_{rr}{}^2 + \sigma_{\theta\theta}{}^2 + \sigma_{zz}{}^2 \tag{9}$$

$$m_a = \frac{\sin\varphi}{\sqrt{3}(3+\sin^2\varphi)}\ ,\ k_1 = \frac{\sqrt{3}c\cos\varphi}{(3+\sin^2\varphi)} \tag{10}$$

Where φ is the internal frictional angle, c is the cohesion stress. σ_{rr}, $\sigma_{\theta\theta}$, σ_{zz} are the principle stress in the cylindrical coordinate system.

3. The numerical simulation model

3.1 The establishment of numerical simulation model

The three-dimensional wellbore stability model which overall considering the effects of fully coupled thermo-poroelastoplasticity and filter cake is established in this paper which consists of 8904 three-dimensional fully coupled temperature–pore pressure elements, just as Fig. 2 shows.

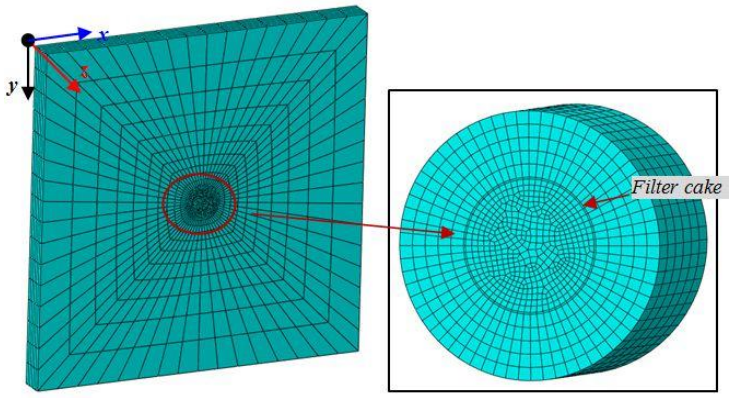

Fig. 2 Finite element used in the computations

Table 1 Properties of the rock used in the computations

Young's modulus, E	2000 MPa
Poisson's ratio, u	0.2
Lame constant, λ	555 MPa
Permeability coefficient, K	1×10^{-12} m·s^{-1}
Porosity, n	0.2
Solid mass density, ρ_m	2350 kg/m^3
Solid mass thermal expansion coefficient, β_m	1.5×10-5 /℃
Solid mass thermal conductivity, k_m	3.08 J/m·s·℃
Solid mass specific heat capacity, c_m	896 J/g·℃
Biot coefficient, α	1
Pore fluid conductivity, k_f	0.58 J/m·s·℃
Pore fluid specific heat capacity, c_f	4200 J/g·℃
Pore fluid thermal expansion coefficient, β_f	2×10^{-4} /℃
Pore fluid density, ρ_f	1000 kg/m^3
Specific weight of pore fluid, γ_w	1×10^4 N/m^3
Fluid viscosity, μ	0.001 Pa·s
Shear modulus, G	833 MPa
Cohesion stress, c	8 MPa
Friction angle, φ	30°

The wellbore stability problem becomes more complex with the coupled effects of pore pressure, in-situ stress, mud pressure and temperature. Abolmaali and Kararam (2009) through the research of the effect of model thickness on tangential stress have found that the less effect of model thickness on tangential stress and strain if the thickness larger than 300 mm, thus the model thickness in this paper is 300 mm. The lengths of model should be ten times bigger than wellbore radius. Taking the wellbore center as the coordinate origin, the boundary condition is $u_z|_{z=150} = u_z|_{z=-150=0}$. The temperature of wellbore wall is equal to the drilling mud and the pore pressure at wellbore wall is equal to the drilling mud pressure after the borehole generation. The properties of the rock are shown in Table 1.

The numerical simulation process can be divided into three steps: the first step is initial ground stress balance calculation; the rock suffers maximum horizontal principal stress, minimum horizontal principal stress and initial pore pressure in this step. The second step is the fully coupled thermo-poroelastoplasticity analysis after the borehole generated by using birth-death element method, in this step, the wellbore suffers the mud pressure and the temperature boundary and pore pressure boundary of wellbore wall will be changed. The third step is the fully coupled thermo-poroelastoplasticity analysis after filter cake forms on the wellbore wall. In this state, the pore pressure boundary of the wellbore wall will be changed again, because the wellbore wall transforms into impermeable from the permeable.

3.2 Verification of numerical simulation model

In order to verify the numerical simulation results, the numerical results were compared to the analytical solutions of the thermo-poroelastic theory, just shown in Eqs. (11) and (12) (Chen and Ewy 2005). The temperature and pore pressure distributions are shown in Figs. 3 and 4. There exist a slight error between numerical results and analytical solutions. The comparison of the two types solutions demonstrate the validity of the numerical simulation model to some extent, thus the further researches were done in this paper are based on this numerical simulation model.

$$T(r,t) = T_0 + (T_w - T_0)\sqrt{\frac{r_w}{r}}erfc(\frac{r - r_w}{2\sqrt{c_0 t}}) \tag{11}$$

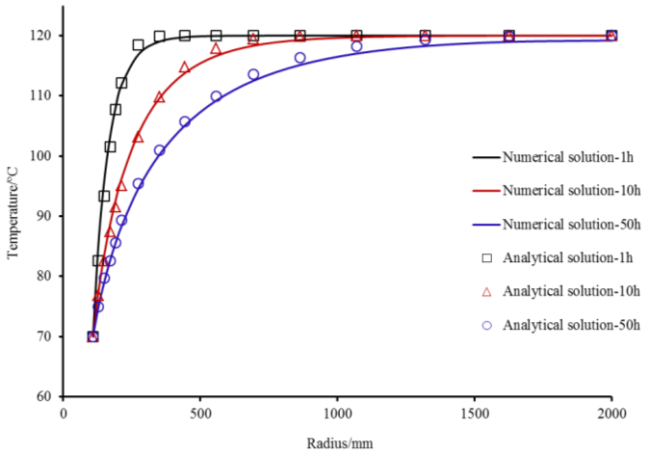

Fig. 3 Numerical and analytical temperature distributions

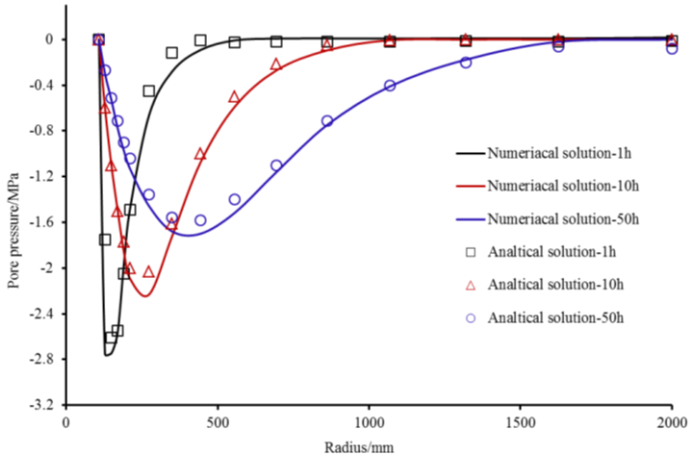

Fig. 4 Numerical and analytical pore pressure distributions

$$p(r,t) = p_0 + (p_w - p_0)\sqrt{\frac{r_w}{r}}erfc(\frac{r-r_w}{2\sqrt{ct}}) - \frac{c^{'}(T_w(t)-T_0)}{1-c/c_0}\sqrt{\frac{r_w}{r}}(erfc(\frac{r-r_w}{2\sqrt{ct}}) - erfc(\frac{r-r_w}{2\sqrt{c_0 t}})) \quad (12)$$

Where, T_0 is the initial temperature of formation; T_w is the temperature of drilling mud; r_w is the wellbore radius; c_0 is the hydraulic diffusivity coefficient; p_0 is the initial pore pressure of formation; p_w is the drilling mud pressure; c is the thermal diffusivity; c' is the thermo-hydraulic coupling coefficient; r is the distance to the center of wellbore.

4. Borehole pore pressure and stress analysis

The drilling fluid will invasion into the wellbore wall or the pore fluid will seep into the borehole after the drilled-out rocks replaced by the drilling mud, resulting in the pore pressure changes. Besides, heat transfer will happen between the drilling mud and wellbore due to its difference. The drilling mud temperature is lower than the bottom formation and larger than the upper formation and the temperature has a significant effect on pore pressure. The initial formation temperature, drilling fluid temperature, borehole radius and the in-situ stress are shown in Table 2.

4.1 The effect of time and temperature on pore pressure

The balances of pore pressure and in-situ stress are broken after the borehole forms. It causes

Table 2 Input parameters

Initial temperature, T_0	120℃
Drilling fluid temperature, T_w	70℃ or 170℃
Borehole radius, r_w	108 mm
Mini horizontal principal stress, σ_h	30 MPa
Max horizontal principal stress, σ_H	40 MPa

many wellbore instability problems, such as wellbore collapse and wellbore fracture. Drilling fluid temperature and time play an important role in pore pressure changes.

The pore pressures around the wellbore for various times and temperatures are shown in Fig. 5 and Fig. 6 when P_w = 30 MPa. For the heating cases, a significant pressure increase is generated near the wellbore at early times in θ = 0° direction. With the time increasing the peak of the pore pressure is reduced and moves away from the wellbore. The pore pressure of the far away wellbore is approximately equal to the initial formation pore pressure. The peak of the pore pressure is increased in θ = 90° direction. For the cooling cases, the peak of the pore pressure is lower than the heating in θ = 0° direction; however, a significant pressure decrease is generated near the wellbore in θ = 90° direction, with the time increasing the peak of the pore pressure is increased. In a word, heating increases the pore pressure and cooling reduces the pore pressure. Also with the time increasing the peak of the pore pressure is reduced in θ = 0° direction while it is increase in θ = 90° direction.

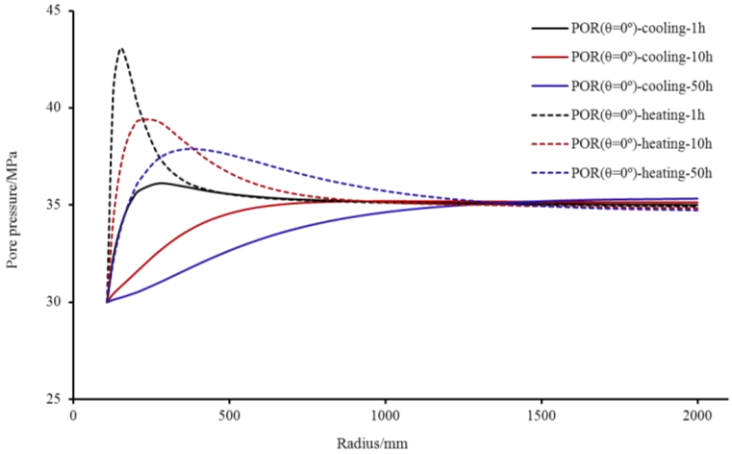

Fig. 5 The distributions of pore pressure in θ = 0° direction

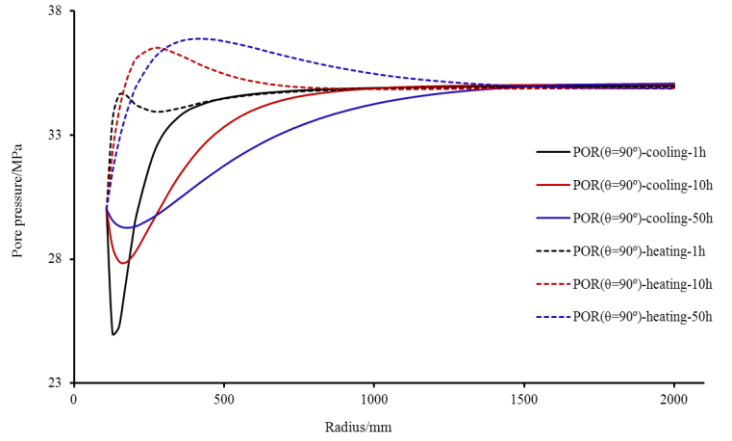

Fig. 6 The distributions of pore pressure in θ=90° direction

4.2 Borehole stress and plastic deformation under different mud pressure

Drilling fluid plays a vital role in keeping wellbore stability during the drilling process. Different drilling fluid pressures will cause different borehole stresses. The shear failure may occurs on wellbore wall since the radial stress (σ_{rr} = S11) is small which caused by the low drilling fluid pressure. What is more, the tensile failure occurs when the tangential force ($\sigma_{\theta\theta}$ = S22) is larger than the tensile strength of wellbore due to the large mud pressure. The compressive stress and tangential stress are supposed to be negative and positive respectively in this paper. The radial stress and tangential stress of wellbore under different drilling fluid pressure after the borehole generated one hour later are shown in Figs. 7-10.

For the cooling cases, the radial stress is compressive stress at wellbore wall in the θ = 0° direction when the drilling mud pressure is equal to 0 MPa. It increases near the wellbore and becomes tensile stress as far away from the wall. The radial stress at wall first increases then

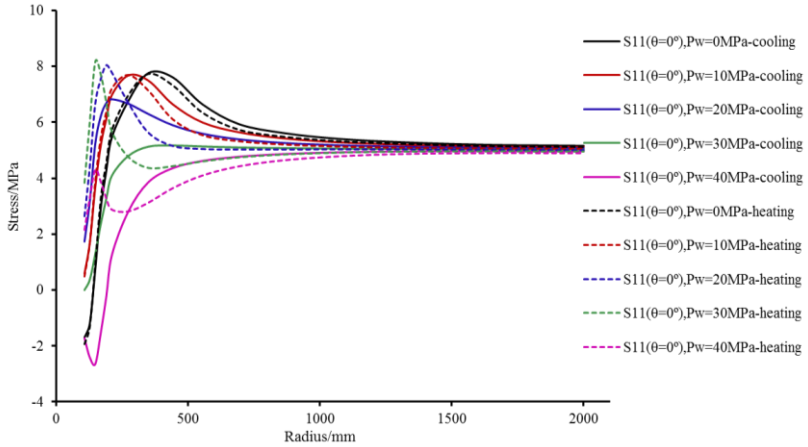

Fig. 7 The distributions of radial stress in the θ = 0° direction

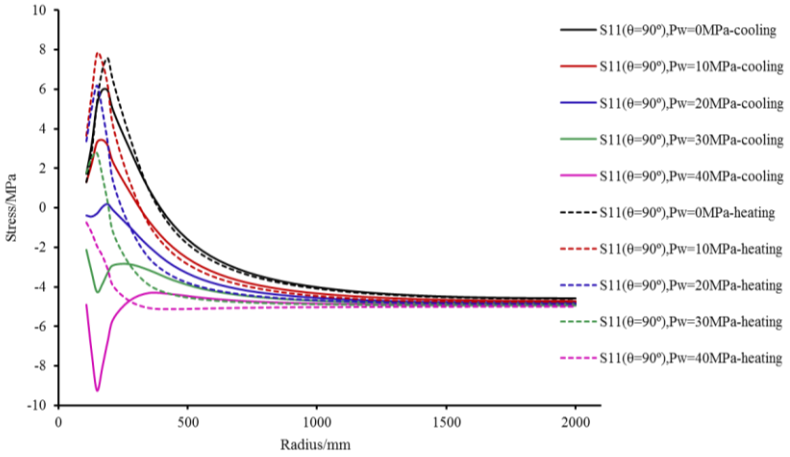

Fig. 8 The distributions of radial stress in the θ = 90° direction

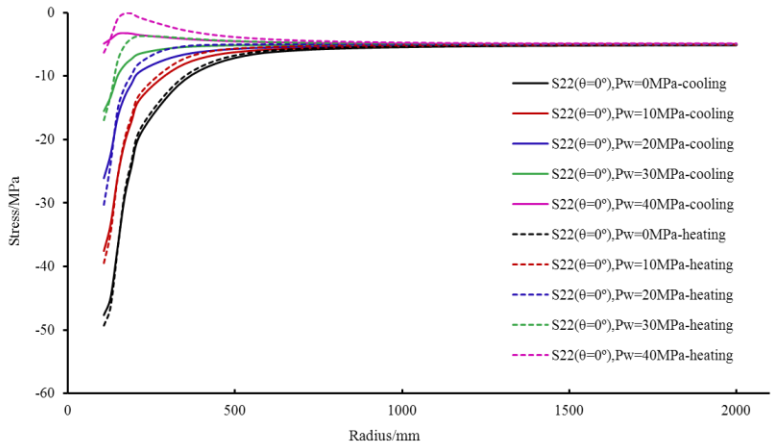

Fig. 9 The distributions of tangential stress in the $\theta = 0°$ direction

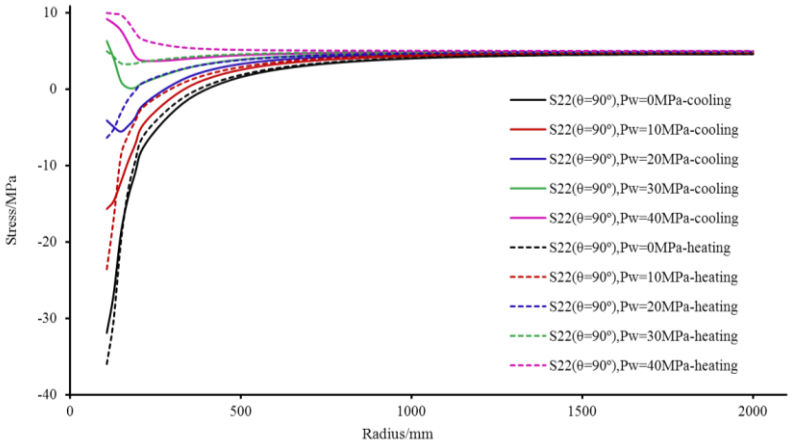

Fig. 10 The distributions of tangential stress in the $\theta = 90°$ direction

decreases as the drilling mud pressure increases while the radial stress peak is decreases. Also, the tangential stress is compressive stress when the drilling mud pressure is equal to 0 MPa and it will increase with the drilling mud pressure increases. The radial stress peak in $\theta = 90°$ direction will decrease as the mud pressure increases, it occurs a negative peak at last, that is mean the radial stress becomes compressive stress from tensile stress. The tangential stress becomes tensile stress from compressive stress with the mud pressure increases, if the tensile stress is larger than the tensile strength of wellbore it occurs tensile failure.

The drilling fluid temperature also has influence on the radial stress and tangential stress, for the heating cases, the radial stress is larger than the cooling cases, but the compressive tangential stress is smaller near the wellbore. The reason for this phenomenon is that the borehole will shrink then the borehole radius increases, so the radial stress is relatively small for the cooling cases, causing tensile tangential stress. Heating increases the radial stress and the expanded borehole causing a compressive tangential stress.

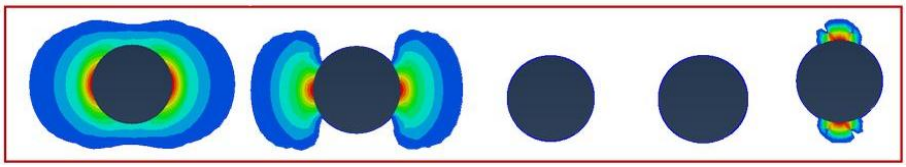

Fig. 11 Plastic deformation for cooling cases under different drilling fluid pressures

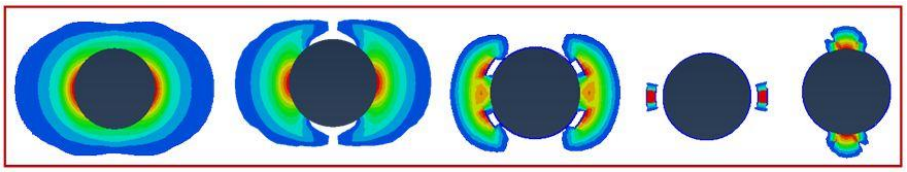

Fig. 12 Plastic deformation for heating cases under different drilling fluid pressures

The plastic deformation of wellbore for the cooling cases and heating cases under different mud pressures after the borehole generated one hour later are shown in Figs. 11 and 12 respectively. Those two pictures more intuitively show the effect of temperature on wellbore stability. The wellbore will happen plastic deformation in the $\theta = 0°$ direction when the mud pressure is low and the plastic zone becomes smaller with the mud pressure increases, as the mud pressure keeping increase the tensile failure happened in the $\theta = 90°$ direction of wellbore. The results show that the safety drilling fluid density window in the cooling cases was much larger than it in heating cases and heating causes a more serious compressive shear failure problem than the cooling in the $\theta = 0°$ direction but the situation of tensile failure in the $\theta = 90°$ direction was not apparent changed for the temperature.

4.3 The borehole stress under various times

The borehole stresses of heating and cooling cases under various times are shown in Fig. 13 and 14 when P_w = 30 MPa. With the time increases, the peak of the radial stress reduces and

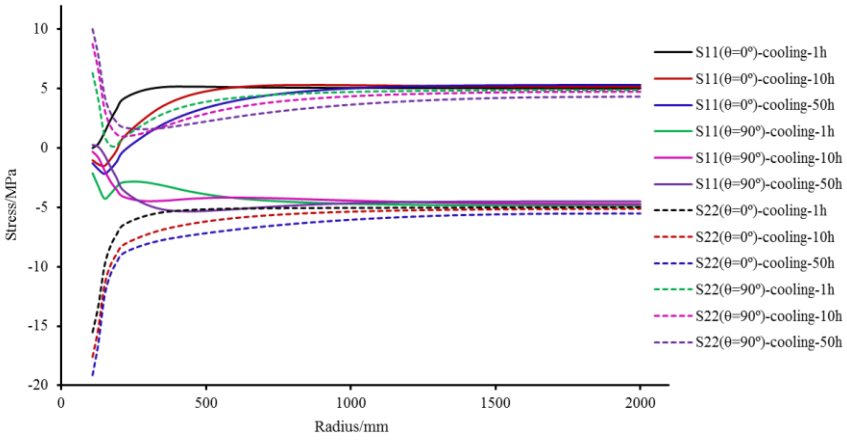

Fig. 13 Borehole stress under various time for cooling cases

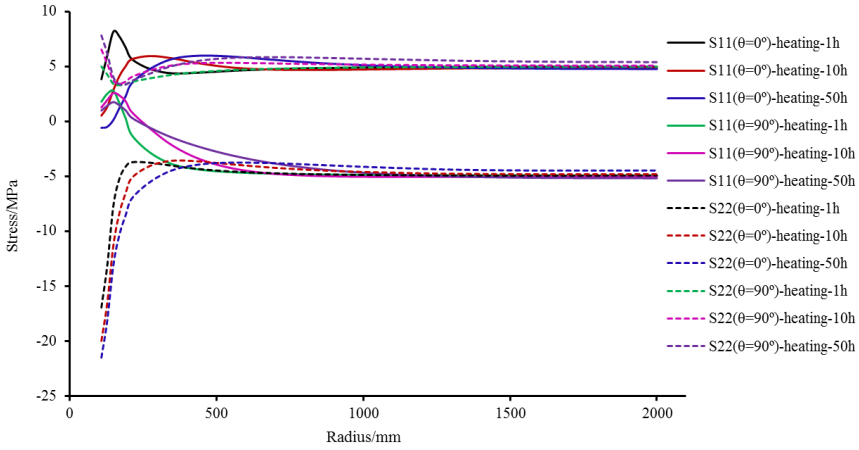

Fig. 14 Borehole stress under various time for heating cases

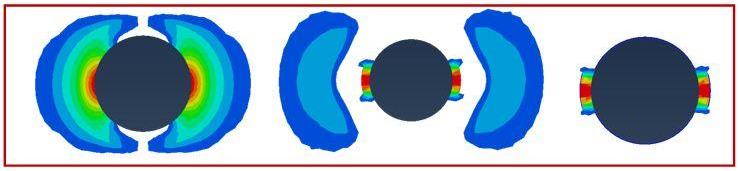

Fig. 15 The plastic deformation under various times for heating cases when P_w=10MPa

moves away from the wellbore in the θ = 0° direction for the cooling cases; the peak of tangential stress decreases with the time increases. The change law of radial stress for the heating cases is the same with the cooling; however, with the time increases the peak of tangential stress has no trend of decrease. For the cooling cases, the radial stress will decrease near the wellbore in θ = 90° direction, the peak of the radial stress will decrease with the time increases and the peak of tangential stress will increase. But for the heating cases, the change law of radial stress is just contrary to the cooling and the change law of tangential stress is the same. In a word, time increase can enhance the tensile failure and relax the shear failure of wellbore. This phenomenon is intuitively shown in Figs. 15 and 20(a).

4.4 The effect of filter cake on wellbore stability

A filter cake can form as quickly as the drilling fluid invasion into the formation while the drilling fluid pressure (40 MPa and 50 MPa are used in this section) is larger than initial pore pressure. The filter cake, which with a much lower permeability and higher shear strength, plays an important role in preventing the drilling fluids seeping into formation and protecting the oil and

Table 3 Physical parameters of filter cake

Young's modulus	Poisson's ratio	density	Filter cake thickness	Friction angle	Cohesion stress
280 MPa	0.3	1.48 g/cm^3	3 mm	25°	0.45 MPa

gas reservoir. It is good for the wellbore stability. Assuming the filter cake formed after borehole generated one hour later. The physical parameters of filter cake are shown in Table 3.

4.4.1 The effect of filter cake on pore pressure

The impermeable boundary occurs if a filter cake forms on the wellbore wall, which prevents drilling fluid seeps into formation and changes the pore pressure near the wellbore. For the cooling cases, the pore pressure at wellbore wall was equal to the drilling fluid pressure before the filter cake generated and the pore pressure decreased near the wellbore. After the filter cake formed, the pore pressure at wellbore changed and the pore pressure at wellbore wall was not equal to the drilling fluid pressure anymore. Just as Fig. 16 shows, the pore pressure at wellbore wall has significantly decreased after the filter cake forms. The main reason is own to the changed boundary of pore pressure.

For the heating cases, the effects of filter cake on pore pressure when the drilling fluid pressure

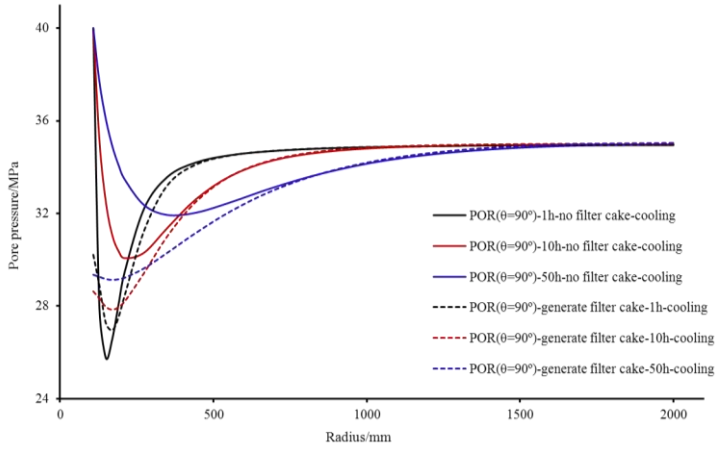

Fig. 16 The effect of filter cake on pore pressures for the cooling cases

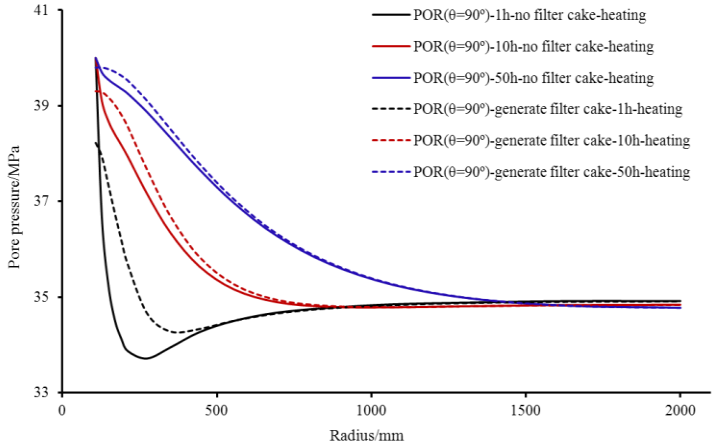

Fig. 17 The effect of filter cake on pore pressures for the heating cases

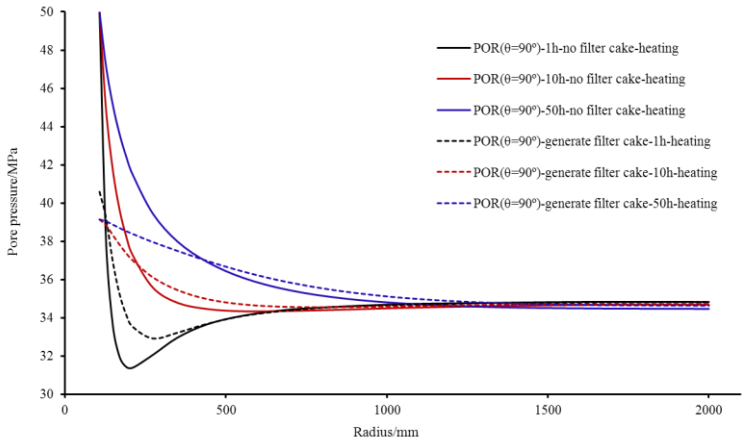

Fig. 18 The effect of filter cake on pore pressures for the heating cases

was equal to 40 MPa or 50 MPa are shown in Figs. 17 and 18 respectively. Form Fig. 18 the pore pressure at wellbore wall was obviously lower because of the generation of filter cake, besides the lower region is become deeper with the time increases. But as Fig. 17 shows, this phenomenon was not apparent. The main reason is that the drilling fluid pressure was almost equal to the initial pore pressure.

4.4.2 The effect of filter cake on tangential stresses

For the cooling cases, the tangential stress of wellbore which with filter cake for the various times is shown in Fig. 19, it was much smaller than the stress without filter cake and the difference between those two situations grown as the time increased. That is to say, the effect of filter cake on tangential stresses got into heavier with the time increased. Fig. 20 more intuitively shows the influence of filter cake on wellbore stability. The wellbore in Fig. 20(a) is without the filter cake while Fig. 20(b) has the filter cake.

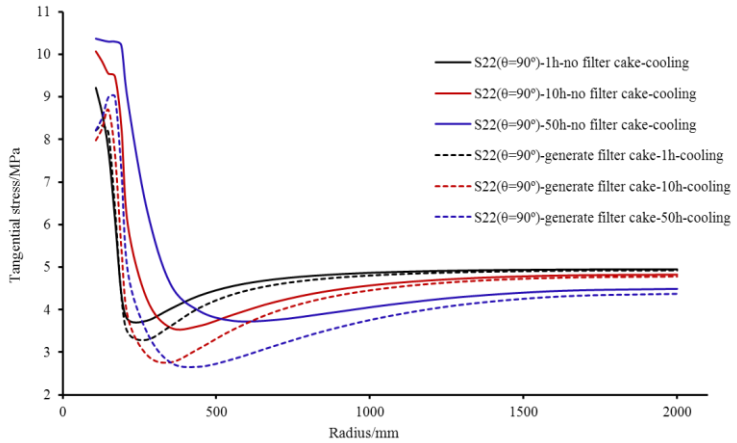

Fig. 19 The effect of filter cake on tangential stress for cooling cases (P_w = 40 MPa)

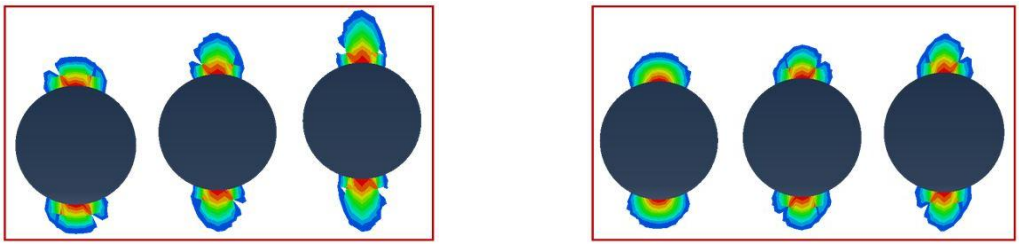

(a) Without filter cake (b) With the filter cake

Fig. 20 The plastic deformation under various times for cooling cases (P_w = 40 MPa)

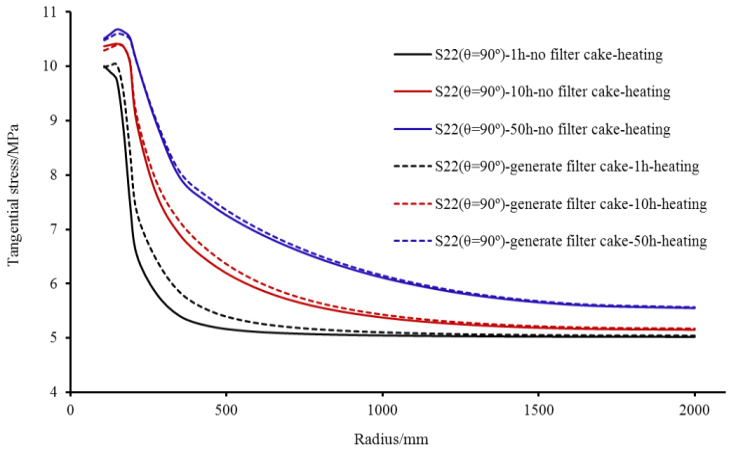

Fig. 21 The effect of filter cake on tangential stress for the heating cases (P_w = 40 MPa)

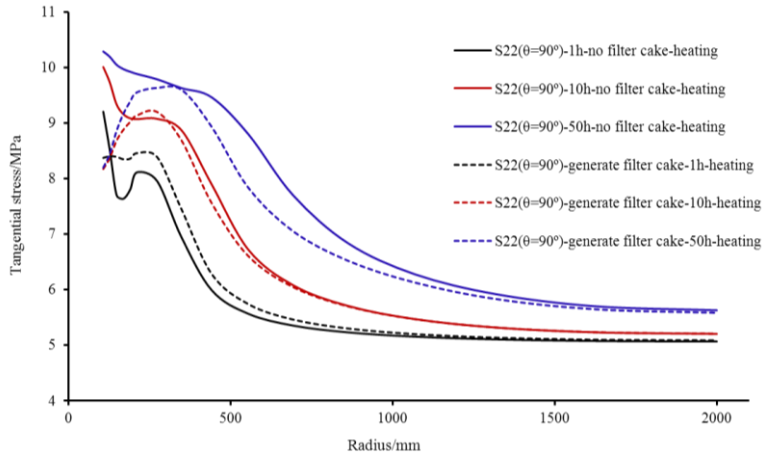

Fig. 22 The effect of filter cake on tangential stress for the heating cases (P_w = 50 MPa)

For the heating cases, the tangential stress of wellbore in θ = 90° direction when the drilling fluid pressure was 40 MPa is shown in Fig. 21. The filter cake had little impact on the tangential

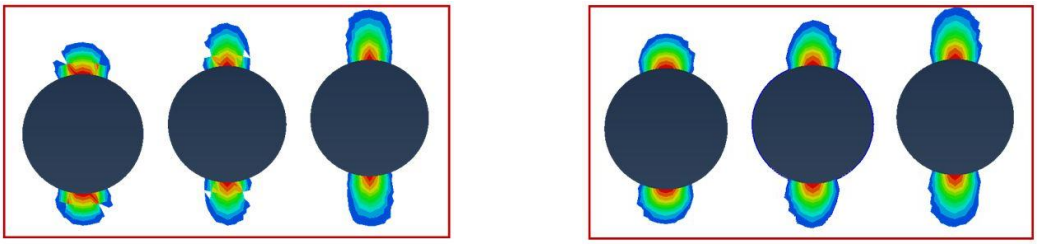

(a) Without filter cake (b) With the filter cake

Fig. 23 The plastic deformation of wellbore for various times (P_w = 40 MPa)

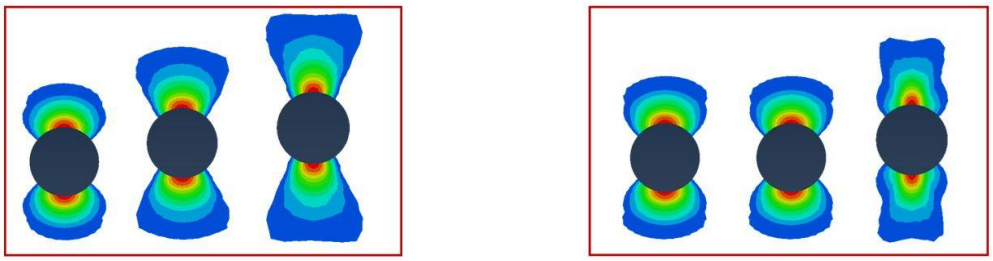

(a) Without filter cake (b) With the filter cake

Fig. 24 The plastic deformation of wellbore for various times (P_w = 50 MPa)

stresses because the drilling fluid pressure was almost equal to the initial pore pressure. Fig. 23 represents the plastic deformation of wellbore for various times.

The tangential stress of wellbore in θ = 90° direction is shown in Fig. 22 as the drilling fluid pressure was 50 MPa. It shows that the tangential stress of the nearby wellbore is reduced increasingly after the filter cake forms especially at the wellbore wall, besides the decreased area is grown deeper with the time increases. Thus the filter cake also plays a crucial role in keeping wellbore stability. The plastic deformation of wellbore for various times is shown in Fig. 24 when the drilling fluid pressure was 50 MPa.

5. Conclusions

The three-dimensional wellbore stability model which overall considering the effects of fully coupled thermo-poroelastoplasticity and filter cake is established based on the finite element method and Drucker-Prager failure criterion. The distribution of pore pressure, wellbore stress and plastic deformation under the conditions of different mud pressures, times and temperatures have been discussed. The results obtained in this paper are as follows.

(1) Heating increases the pore pressure and cooling reduces the pore pressure, with the time increasing the peak of the pore pressure was reduced in θ = 0° direction while it was increase in θ = 90° direction, the pore pressure of the far away wellbore was maintain around the initial formation pore pressure.

(2) The wellbore will happen plastic deformation in the θ = 0° direction when the mud pressure was low and the plastic zone becomes smaller with the mud pressure increases, as

the mud pressure keeping increase the tensile failure happened in the $\theta = 90°$ direction of wellbore. The results show that the safety drilling fluid density window in the cooling cases was much larger than it in heating cases and cooling tends to prevent shear failure, whereas heating can enhance the shear failure and can cause tensile failure by excessive increase of pore pressure, as a result the wellbore instability problem in heating cases was more serious.

(3) With the time increasing the peak of the radial stress reduced and moved away from the wellbore in the $\theta = 0°$ direction for the cooling cases; the peak of tangential stress decreases with the time increases; the change law of radial stress for the heating cases were the same with the cooling; however, with the time increases the tangential stress had no trend of decrease. For the cooling cases, the radial stress will decreased near the wellbore in $\theta = 90°$ direction, the peak of the radial stress will decrease with the time increases and the peak of tangential stress will increase; but for the heating cases, the change law of radial stress was just contrary to the cooling but the change law of tangential stress was the same. In a word, time increase tends to enhance the tensile failure and weaken the shear failure of wellbore.

(4) The formed filter cake can significantly decrease the pore pressure and tangential stress of the nearby wellbore, especially at wellbore wall. It plays a positive role in preventing wellbore from tensile failure, besides, this phenomenon presents more obviously with the time increases.

Acknowledgments

This research is supported by the Natural Science Fund for Outstanding Youth Science Fund (Grant No. 51222406), New Century Excellent Talents in University of China (NCET-12-1061), Scientific Research Innovation Team Project of Sichuan Colleges and Universities (12TD007), Youth Scientific Research Innovation Team Project of Sichuan Province (2014TD0025).

References

Abolmaali, A. and Kararam, A. (2009), "Nonlinear finite-element-based investigation of the effect of bedding thickness on buried concrete pipe", *J. Transport. Eng.*, **136**(9), 793-799.

Biot, M.A. (1941), "General theory of three-dimensional consolidation", *J. Appl. Phys.*, **12**(2), 155-164.

Cai, M.F., He, M.C. and Liu, D.Y. (2002), *Rock Mechanics and Engineering*, Beijing, China.

Chen, G. and Ewy, R.T. (2004), "Thermoporoelastic effect on wellbore stresses in permeable rocks", *ARMA-04-467*, *Proceedings of the 6th North America Rock Mechanics Symposium* (*NARMS*), *American Rock Mechanics Association*, Houston, TX, USA, June.

Chen, G., Chenevert, M.E., Sharma, M.M. and Yu, M. (2003), "A study of wellbore stability in shales including poroelastic, chemical, and thermal effects", *J. Petrol. Sci. Eng.*, **38**(3), 167-176.

Cui, L., Cheng, A.H.D. and Abousleiman, Y. (1997), "Poroelastic solution for an inclined borehole", *J. Transport. Eng.*, **64**(1), 32-38.

Cui, L., Ekbote, S., Abousleiman, Y. and Zaman, M.M. (1998), "Borehole stability analyses in fluid saturated formations with impermeable walls", *Int. J. Rock Mech. Min. Sci.*, **35**(4), 582-583.

Cui, L., Abousleiman, Y., Cheng, A.H. and Roegiers, J.C. (1999), "Time-dependent failure analysis of inclined boreholes in fluid- saturated formations", *J. Energy Resour. Technol.*, **121**(1), 31-39.

Chen, G. and Ewy, R.T. (2005), "Thermoporoelastic effect on wellbore stability", *SPE Journal*, **10**(2), 121-129.

Chen, M., Jing, Y. and Zhang, G.Q. (2008), *Petroleum Engineering Rock Mechanics*, Beijing, China.
Detournay, E. and Cheng, A.H.D. (1988), "Poroelastic response of a borehole in a non-hydrostatic stress field", *Int. J. Rock Mech. Min. Sci. Geomech. Abstracts*, **25**(3), 171-182.
Diek, A., White, L., Roegiers, J.C. and Blankenship, D. (2012), "A fully coupled thermoporoelastic model for drilling in HPHT formations", *Proceedings of the 12th ISRM Congress, International Society for Rock Mechanics*, Beijing, China, October.
Gelet, R., Loret, B. and Khalili, N. (2012), "Borehole stability analysis in a thermoporoelastic dual-porosity medium", *Int. J. Rock Mech. Min. Sci*., **50**(1), 65-76.
Gomar, M., Goodarznia, I. and Shadizadeh, S.R. (2014), "A transient fully coupled thermo-poroelastic finite element analysis of wellbore stability", *Arab. J. Geosci*., **8**(6), 3855-3865.
Jia, S., Ran, X., Wang, Y., Xiao, T. and Tan, X. (2012), "Fully coupled thermal-hydraulic-mechanical model and finite element analysis for deformation porous media", *Chinese J. Rock Mech. Eng*., **31**(supp.2), 3547-3556.
Muller, A.L., do Amaral Vargas, E., Vaz, L.E. and Goncalves, C.J. (2009), "Three-dimensional analysis of boreholes considering spatial variability of properties and poroelastoplasticity", *J. Petrol. Sci. Eng*., **68**(3), 268-276.
Palciauskas, V.V. and Domenico, P.A. (1982), "Characterization of drained and undrained response of thermally loaded repository rocks", *Water Resour. Res*., **18**(2), 281-290.
Rice, J.R. and Cleary, M.P. (1976), "Some basic stress diffusion solutions for fluid-saturated elastic porous media with compressible constituents", *Review. Geophys*., **14**(2), 227-241.
Santarelli, F.J., Brown, E.T. and Maury, V. (1986), "Analysis of borehole stresses using pressure-dependent, linear elasticity", *Int. J. Rock Mech. Min. Sci. Geomech. Abstracts*, **23**(6), 445-449.
Shahabadi, H., Yu, M., Miska, S.Z., Takach, N.E. and Chen, G. (2006), "Modeling transient thermo-poroelastic effects on 3D wellbore stability", *SPE 103159*, *Proceedings of SPE Annual Technical Conference and Exhibition*, San Antonio, TX, USA, September.
Sheng, J.C., Liao, Q.L., Liu, J.S. and Baoyu, S.U. (2008), "Analysis of coupled porothermoelastic response of a wellbore by using a femlab-based simulator", *Eng. Mech*., **25**(2), 219-223.
Sheng, J.C., Liu, J.S., Xu, X.C. and Zhan, M.L. (2009), "A coupled porochemothermoelastic model for a borehole in shales", *Eng. Mech*., **26**(12), 240-245.
Tao, Q. and Ghassemi, A. (2010), "Poro-thermoelastic borehole stress analysis for determination of the in situ stress and rock strength", *Geothermics*, **39**(3), 250-259.
Wang, Y. and Dusseault, M.B. (2003), "A coupled conductive–convective thermo-poroelastic solution and implications for wellbore stability", *J. Petrol. Sci. Eng*., **38**(3), 187-198.
Wang, X., Cheng, Y. and Zhao, Y. (2007), "The effect of temperature on wellbore stability in shales during drilling", *Petrol. Drill. Techniq*., **35**(2), 42-45.
Wang, M., Zhang, Z. and Ma, Q. (2014), "Influence of thermo-seepage coupling effect on wellbore stress under the underbalanced condition", *Drill. Production Technol*., **37**(1), 1-3.
Wu, C., Chen, M. and Jin, Y. (2009), "A prediction method of borehole stability based on seismic attribute technology", *J. Petrol. Sci. Eng*., **65**(3-4), 208-216.
Zhai, Z., Zaki, K.S., Marinello, S.A. and Abou-Sayed, A.S. (2009), "Coupled thermoporomechanical effects on borehole stability", *SPE 123427*, *Proceedings of SPE Annual Technical Conference and Exhibition*, New Orleans, LA, USA, October.
Zhang, J., Lang, J. and Standifird, W. (2009), "Stress, porosity, and failure-dependent compressional and shear velocity ratio and its application to wellbore stability", *J. Petrol. Sci. Eng*., **69**(3), 193-202.
Zhu, X. and Liu, W. (2013), "The effects of drill string impacts on wellbore stability", *J. Petrol. Sci. Eng*., **109**, 217-229.
Zhu, Y.W., Cai, Y.Q. and Xu, H. (2005), *ABAQUS and Analyses of Rock Engineering*, Hong Kong.

CC